Diffusion trajectory of an asymmetric object: Information overlooked by the mean square displacement

Claire Ribrault* and Antoine Triller†
Inserm, U789, Biologie Cellulaire de la Synapse N&P, Paris, France
and Ecole Normale Supérieure, Paris, France

Ken Sekimoto‡
UMR MSC CNRS-Paris 7 7057, and UMR Gulliver, CNRS-ESPCI 7083, Paris, France
(Received 10 November 2006; published 14 February 2007)

Diffusion of an asymmetric object is characterized by its translational and rotational diffusion coefficients. Until now, anisotropic diffusion studies have been based on ensemble averages. Here we present a theoretical basis for the analysis of the trajectories of a single particle with anisotropic diffusion coefficients. We discuss the relevance of this method for motion of biomolecules in the membrane of living cells.

DOI: 10.1103/PhysRevE.75.021112 PACS number(s): 05.40.Jc, 82.37.Rs, 46.65.+g

I. INTRODUCTION

Experimental studies of diffusion of particles have originally been carried out by using methods that measure the average behavior of an entire population, such as dynamic light scattering [1] or neutron scattering [2] in physics, or fluorescence recovery after photobleaching (FRAP) [3] or fluorescence correlation spectroscopy (FCS) [4] commonly used in biology. For 20 years now, optical methods have been developed for observing the motion of single particles [5,6]. These methods, referred to as single particle tracking (SPT) methods, consist in following the trajectory of a marker attached to the diffusing molecule. Transport properties of the particle are then derived through a statistical analysis of the trajectory, that includes, for instance, measurement of the mean square displacement. SPT methods thereby provide information not available through measurements of the properties of large ensembles of particles.

Visualization of the diffusive behavior of single membrane proteins in living cells has revealed that these molecules undergo a variety of motions, such as Brownian, confined, or directed motion [6,7]. In this context, SPT is a powerful tool for investigating the membrane structure and the mechanisms responsible for these motions, which ultimately influence reactions and interactions between biomolecules [8]. Current analyses of trajectories allow the determination of the translational diffusion coefficient of a symmetric molecule which undergoes isotropic diffusion.

However, in a two-dimensional isotropic homogeneous environment, asymmetric molecules have two distinct translational diffusion coefficients, $D_{\parallel}$ for diffusion along the longitudinal (or principal) axis of the particle and $D_{\perp}$ ($D_{\parallel} \geq D_{\perp}$) [9–11] along the transversal axis, and a rotational diffusion coefficient, D_{r} (see Fig. 1).

Since translational mobility is anisotropic, translational and rotational diffusion are coupled. Qualitatively, the slower the rotational diffusion is, the longer the particle will diffuse in the same direction. As a consequence, trajectories of asymmetric molecules differ from those of symmetric ones as is illustrated by Fig. 2. A method of analyzing the motion of single anisotropic molecules was developed by Perrin [12,13]. Motivated by the recent development of SPT methods, we revisit this issue and focus on the trajectories of a single anisotropic molecule. In this study, we propose a method to deduce the translational and rotational diffusion coefficients of an asymmetric object diffusing in a two-dimensional space from the trajectory of its pointlike marker.

Our strategy has been to solve the evolution or Langevin equation, which has allowed calculation of the exact analytical expressions of some statistical quantities, that characterize the geometry of the trajectory. This analytical method is more powerful than those based on the characterization of collective properties of an ensemble of particles: the latter require knowledge of the probability distribution function, which cannot be analytically determined [14–16], and therefore are based on a perturbation approximation and are only valid for weakly asymmetric particles [16].

We present below the Langevin equation for a single asymmetric object, then the statistical functions obtained from ensembles of trajectories from which we can determine the diffusion coefficients. In the last section we discuss the relevance of this theoretical approach in a biological context.

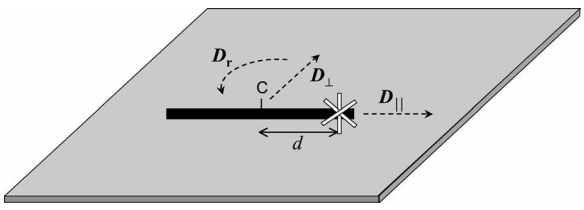

FIG. 1. Definition of principal axes of the translational diffusion coefficients, $D_{\parallel}$ and $D_{\perp}$, and the rotational diffusion coefficient, D_r, around the center of diffusion (C; position $\vec{X}^{(0)}$). The marker (asterisk, position $\vec{X}$) is at a distance d off the center along the longitudinal direction.

*Electronic address: claire.ribrault@ens.fr
†Electronic address: triller@biologie.ens.fr
‡Electronic address: ken.sekimoto@espci.fr

II. DYNAMICS OF DIFFUSING ANISOTROPIC OBJECT ON A PLANE

$D_\parallel$ and $D_\perp$ are the translational diffusion coefficients corresponding, respectively, to the longitudinal and transverse axes of the object, and D_r is the rotational diffusion coefficient. For simplicity of the calculation, we first describe the motion of the center of diffusion (CD), which is the appropriate point to which translational and rotational quantities must be referred [17]. We denote by $\vec{X}_t^{(0)}=(X_t^{(0)},Y_t^{(0)})$ the position of the CD of the diffusing object in the xy plane, and by ϕ_t the angle made by the longitudinal axis and the positive x axis.

An extension of simple Brownian motion leads to the following coupled equations [18]:

$$\frac{\mathrm{d}}{\mathrm{d}t}\begin{bmatrix} X_t^{(0)} \\ Y_t^{(0)} \end{bmatrix} = \begin{bmatrix} \sqrt{2D_\parallel}\cos^2\phi_t + \sqrt{2D_\perp}\sin^2\phi_t & (\sqrt{2D_\parallel}-\sqrt{2D_\perp})\cos\phi_t\sin\phi_t \\ (\sqrt{2D_\parallel}-\sqrt{2D_\perp})\cos\phi_t\sin\phi_t & \sqrt{2D_\parallel}\sin^2\phi_t + \sqrt{2D_\perp}\cos^2\phi_t \end{bmatrix}\begin{bmatrix} \Theta_{x,t} \\ \Theta_{y,t} \end{bmatrix}, \tag{1}$$

where the angle ϕ_t evolves with

$$\frac{d\phi_t}{dt} = \sqrt{2D_r}\xi_t. \tag{2}$$

The random forces, $(\Theta_{x,t},\Theta_{y,t},\xi_t)$, are assumed to be independent correlation-free Gaussian random noises satisfying $\langle\Theta_{x,t}\rangle=\langle\Theta_{y,t}\rangle=\langle\xi_t\rangle=0$, and $\langle\Theta_{x,t'}\Theta_{x,t}\rangle=\langle\Theta_{y,t'}\Theta_{y,t}\rangle=\langle\xi_{t'}\xi_t\rangle=\delta(t'-t)$. The Langevin equations can be solved analytically since the evolution of ϕ_t is obtained by solving separately (2) (see the Appendix A). The position of the marker, $\vec{X}_t=(X_t,Y_t)$, is then obtained by

$$X_t = X_t^{(0)} + d\cos\phi_t, \quad Y_t = Y_t^{(0)} + d\sin\phi_t, \tag{3}$$

where d specifies the distance between the CD and the marker along the longitudinal axis (generalization to other positions of the marker is in principle feasible). Our method allows the determination of this distance d, while the exact position of the marker is not known in classical SPT experiments. We also note that the probability distribution function still cannot be determined because it requires the average over infinitely many moments ($\langle\vec{X}_t\rangle$, $\langle\vec{X}_t\vec{X}_t\rangle$, $\langle\vec{X}_t\vec{X}_t\vec{X}_t\rangle$, etc.).

In addition, the trajectories of the marker based on these equations can readily be simulated. Simulations will allow the estimation of the number of trajectories required for an accurate assessment of the diffusion coefficients. Details of the numerical method used are summarized in the Appendix C.

We define the following characteristic length and time scales,

$$\ell = \left(\frac{D_\parallel + D_\perp}{2D_r}\right)^{1/2}, \quad \tau = (D_r)^{-1}. \tag{4}$$

The above Langevin equations can then be nondimensionalized (see the Appendix A), where the anisotropy of the particle is characterized by a parameter η, which takes a value between 0 and 1,

$$\eta = (D_\parallel - D_\perp)/(D_\parallel + D_\perp). \tag{5}$$

Qualitatively, the particle does not appreciably change its orientation until it diffuses along a distance $\sim\ell$ for time $\sim\tau$. Then, for large η (e.g., Ref. [19]), the particles which are initially randomly oriented but spatially localized around the origin will become oriented along the radial direction of their displacements at short time. See (6) and Fig. 2.

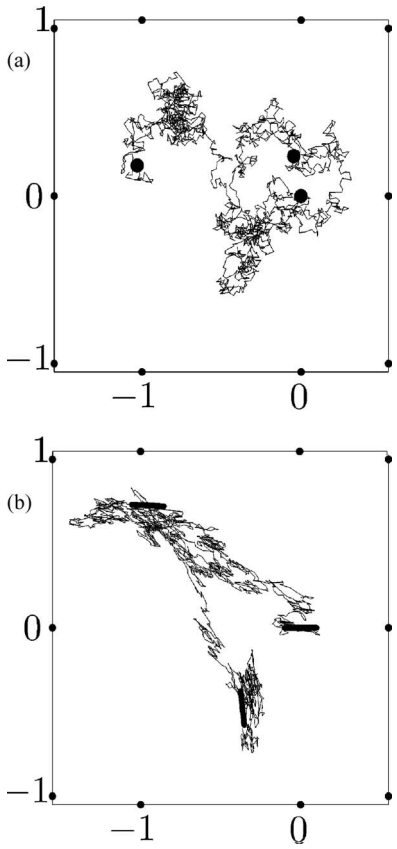

FIG. 2. Examples of trajectories of symmetric (a) and asymmetric (b) particles generated numerically. The marker on the particle is placed at the center of diffusion ($d=0$). The thick black symbols represent the position of the particle at $t=0$ [at the origin (0,0)], $t=\tau/2$, and $t=\tau$. The principal diffusion coefficients are chosen to be $(D_\parallel,D_\perp,D_r)=(1,1,1/2)$ (a) or $(1,1/10,1/2)$ (b), in the length units of ℓ and the time unit of τ. Spatial coordinates are also represented in units of ℓ. The time step of calculation is chosen to be $\Delta t=\tau/200$.

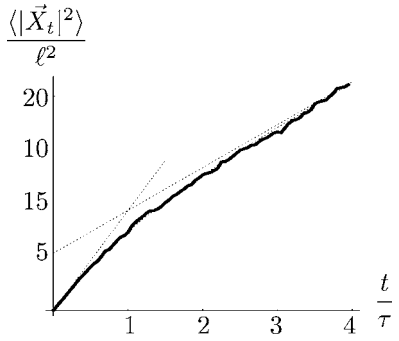

FIG. 3. Comparison of the simulated mean square displacements (MSD), $\langle|\vec{X}_t-\vec{X}_0|^2\rangle$ ($d\neq 0$) using 600 trajectories (thick curve) with the analytical result (dashed curve). The dashed lines are the initial and final asymptotes. Except for the off-center distance of the marker chosen, $d=2\ell$, the result is completely scaled by the characteristic length ℓ and time τ, irrespective to the anisotropy parameter, η. The time step of calculation is chosen to be $\Delta t=\tau/20$.

III. STATISTICAL PROPERTIES OF TRAJECTORIES

From the solution of the Langevin equations, we are able to calculate statistical quantities that characterize the motion of the particle and thereby derive its diffusion coefficients. The analytical expressions of those quantities are presented in the Appendix B. In the analysis below we assume that the origin is at the initial position of the CD, $(X_0^{(0)},Y_0^{(0)})=(0,0)$, and that the initial angle, ϕ_0, is homogeneously distributed over the entire angle, $[0,2\pi]$.

First, the mean square displacement (MSD) $\langle|\vec{X}_t-\vec{X}_0|^2\rangle$ as a function of time is shown in Fig. 3.

The MSD depends on ℓ, and if d is nonzero, of d and τ. It is, however, independent on the anisotropy parameter η. In particular, if the marker is fixed at the CD of the particle, the observed MSD is linear, even though the particle is asymmetric. When the marker is not located at the CD, the MSD exhibits an initial transient that allows the determination of the characteristic time τ. The initially greater slope of the MSD is attributed to the displacement of the marker due to the rotation of the particle (which is not negligible compared to the initial small displacements due to translational diffusion), while the final slope represents only the translational diffusion. The latter asymptote is offset from the origin by $2d^2$, which results from the uncorrelated rotational fluctuations at the initial and final time, ϕ_0 and ϕ_t, respectively.

Then the anisotropy parameter η remains to be determined. Equation (1) shows that the spatial motion of the CD is not a Markov process, in the sense that the probability of a position at a future time, t_1, is not completely specified by the position at present time $t_0(<t_1)$, but also depends on the orientation of the particle at t_0.

Such a correlation between the orientation of the displacement of the particle, $\vec{X}_t^{(0)}$, and that of the diffusing particle itself, $\hat{u}_t$, can be expressed by the following function:

$$\hat{C}(t)=\langle[\vec{X}_t^{(0)}\cdot\hat{u}_t]^2\rangle-\tfrac{1}{2}\langle|\vec{X}_t^{(0)}|^2\rangle, \tag{6}$$

where $\vec{p}\cdot\vec{q}$ denotes the scalar product. This quantity is shown in Fig. 4(a) for several values of η. The result can be interpreted as follows: For $t<\tau$ the orientation $\hat{u}_t$ has undergone only small fluctuations with respect to the initial one, $\hat{u}_0$, and the diffusive displacement, $\vec{X}_t^{(0)}$, is more or less directed along $\hat{u}_0$. The analytical expression of this quantity allows determining the anisotropy parameter. However, classical SPT experiments do not reveal the orientation of the diffusing particle (see the Discussion). We propose the following function $C(0,t,t')$ to express the translation-rotation coupling in terms of the observable displacement $\vec{X}_t$ only,

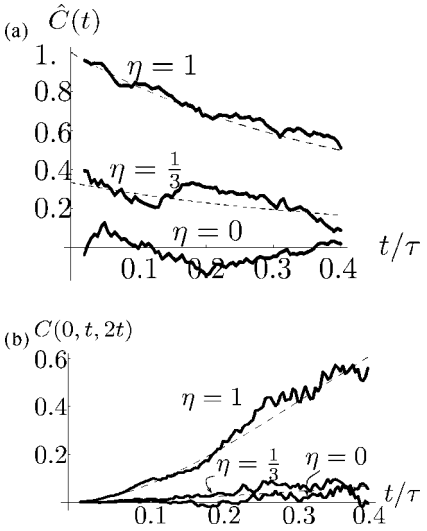

FIG. 4. Cross correlation between the displacement and particle orientation, $\hat{C}(t)$ (a), and persistence of the diffusing direction $C(0,t,2t)$ (b). See (6) and (7), respectively, for the definitions. The functions are presented vs t/τ for various values of the anisotropy parameter, $\eta=0$ (bottom), 1/3 (middle), 1 (top). The off-center distance of the marker was chosen to be $d=0$. Analytical results (dashed curves) are compared with the simulated data over 600 trajectories (thick curves). In (b) the calculation is truncated at $t=0.4\tau$ since, with the present time step of calculation ($\Delta t=\tau/600$), the accuracy becomes poor beyond this point [due mainly to the fact that the function $C(0,t,2t)$ is a subtle difference between two growing terms of $\sim t^2$].

$$C(0,t,t')=2\langle[(\vec{X}_t-\vec{X}_0)\cdot(\vec{X}_{t'}-\vec{X}_t)]^2\rangle-\langle|\vec{X}_t-\vec{X}_0|^2|\vec{X}_{t'}-\vec{X}_t|^2\rangle, \tag{7}$$

with $0<t<t'$. Up to time $\sim\tau$ this quantity gives an estimation of the persistence of the diffusing direction, see Fig. 4(b).

In principle, the translational and rotational diffusion coefficients and the off-center distance can be derived from the MSD and the function $C(0,t,t')$. The $\langle|X_t|^4\rangle$ has also been shown to depend on the anisotropy parameter η, but with such a subtle dependence that it does not allow deduction of the diffusion coefficients. The analytical result of $\langle|\vec{X}_t|^4\rangle$ (see the Appendix B) however, shows clearly that the position $\vec{X}_t$ does not obey a Gaussian distribution since it does not satisfy $\langle|X_t|^4\rangle=2\langle|X_t|^2\rangle^2$.

IV. DISCUSSION

In this paper we have developed a theoretical approach for two-dimensional diffusion of asymmetric objects in an isotropic homogeneous environment. We have focused our analysis on trajectories of a pointlike marker attached to a single diffusing particle. In particular, we have shown how the translation-rotation coupling can be uncovered using new statistical functions obtainable from these trajectories. From this analysis we have established a method to derive the diffusion coefficients of an asymmetric particle from the trajectory of a pointlike marker. We have shown that diffusion anisotropy, η, cannot be approached using the MSD: the MSD depends only on the characteristic time $\tau=(D_r)^{-1}$, the characteristic length $\ell=[(D_\parallel+D_\perp)/(2D_r)]^{1/2}$, and the off-center distance of the marker with respect to the center of diffusion, d. Analyses of trajectories of diffusing membrane proteins (obtained by SPT) are usually based on MSD measurements only and, therefore, are not able to give any information about the anisotropy of the trajectory. We have established an additional statistical function, $C(0,t,2t)$ (defined in the text) that allows the determination of the anisotropy parameter $\eta=(D_\parallel-D_\perp)/(D_\parallel+D_\perp)$. Therefore, when the $C(0,t,2t)$ is combined with the MSD analysis, the three diffusion coefficients ($D_\parallel$, $D_\perp$, and D_r) can be determined. This framework can be generalized to the three-dimensional case: the mathematical structure of the Langevin equation is common to the two-dimensional case since the orientation of the particle evolves separately from that of the position vector $\vec{X}_t$. Practically, however, the complexity of calculations is higher in three dimensions because of the noncommutativity of rotations of three-dimensional objects [20].

From an experimental point of view, the accuracy of the determination of the diffusion coefficients depends on at least three conditions.

First, in the method we propose, the determination of the diffusion coefficients is based on statistical averages. We have not calculated the statistical error, due to the finite number of analyzed trajectories. In order to estimate the number of trajectories required to assess the diffusion coefficients, we performed numerical simulations. (Temporal discretization of Langevin equation introduces another type of error, which is discussed in the Appendix C.) These simulations indicate that a fairly good estimation of the parameters (see Figs. 3 and 4) is obtained with only a few hundreds trajectories analyzed on a time interval $t\sim\tau/2$. Such a number of trajectories can be experimentally obtained.

Second, if the orientation of a particle can be directly accessed, the rotational diffusion coefficient can be indepedently determined. This would facilitate the estimation of the anisotropy parameter η, through, for example, the function $\hat{C}(t)$ [see (6)]. Recently, a method based on the analysis of the light emission pattern of quantum dots (inorganic fluorescent markers [6]) has been developed to observe their orientation [21]. In another technique, two markers are attached to the diffusing particle and their relative positions inform about the orientation of the diffusing object [22]. The rotational diffusion coefficient could also be estimated by methods measuring the average behavior of the particle, such as time resolved fluorescence anisotropy measurements for instance [23].

Third, the spatial and temporal resolutions of the techniques used for the observation of trajectories are of critical importance: they should be higher than the characteristic length and time, beyond which anisotropy is practically not appreciable. Various experimental methods such as FRAP or SPT allow determination of isotropic diffusion coefficients of symmetric membrane proteins. Based on these values, we estimate the order of magnitude of anisotropic diffusion coefficients of asymmetric membrane proteins. The characteristic length and time would be $\ell\sim 1$ nm and $\tau\sim 10$ μs, taking $D_\parallel=0.2$ $\mu m^2/s$ (for membrane proteins in model bilayers [10]), $D_\parallel/D_\perp=2$ (representative ratio for 3D Brownian motion in Newtonian fluids, which depends on the properties of the environment and on the particle geometry [11]), and $D_r=10^5$ s^{-1} [24]. The spatio-temporal resolutions compatible with these characteristic parameters are beginning to be available [25–27].

Below, we discuss the relevance of this study for the diffusion of proteins in membranes of living cells.

The model we have presented is valid for particles diffusing in a homogeneous isotropic environment. This is not the case at all scales for biological membranes of living cells. The cell membrane (i) contains various membrane proteins that can either act as traps by transiently immobilizing the diffusing particle or as obstacles by hindering its diffusion [25], (ii) contains lipid microdomains, the size of which can range from tens to hundreds of nanometers [28], and (iii) is further compartmentalized with domains as large as a few hundreds nanometers in diameter [25]. This latter compartmentalization results from the existence of corrals formed by membrane proteins anchored to a submembranous cytoskeleton network. This membrane organization should be considered in a context where proteins diffuse and lipid rafts have a finite lifetime. This heterogeneity, whether structured or not, dynamic or not, is likely to affect the diffusion of proteins in the membrane. This heterogeneity can be quantified by a characteristic length below which the membrane is homogeneous and does not contain any obstacle and/or trap for the diffusing protein. The motion of a protein diffusing over such a distance should therefore remain unaffected by membrane heterogeneity. The anisotropic motion we have described in this study therefore might be visible in small homogeneous patches of membranes, i.e., when the observation length scale is small compared to the heterogeneity characteristic length. By contrast, when the protein diffuses over larger distances, its motion will be influenced by interactions with other proteins. Its behavior is expected to deviate from that of proteins diffusing in a homogeneous environment. Modifications of the membrane heterogeneity, for instance by altering the lipid composition or disrupting the actin cytoskeleton responsible for the membrane compartmentalization [25], will then help interpret deviation from the homogeneous membrane model. In addition, simulations of diffusion in crowded environments can also be performed and then compared with experimental data, as has already been done for isotropic particles [25,29]. Preceding simulations [30,31] have shown that the motion of a rod diffusing in an environment that contains fixed obstacles becomes

non-Brownian for a high density of obstacles (that is when the observation length becomes large compared to the heterogeneity characteristic length). Incorporation of the environment heterogeneity and structure into the diffusion model therefore is one of the future tasks to be challenged.

Beyond investigation of the membrane organization, observing the diffusive behavior of membrane proteins could provide a tool for studying interactions between proteins. Protein motion depends on the shape of the protein and especially, as we have shown here, on its anisotropy. Any change in the shape of the diffusing object will then reflect in its trajectory. Proteins can transiently form asymmetric complexes with some of their partners. In some cases, complex formation is induced by a ligand. For instance, tyrosin kinase receptors dimerize in response to ligand binding [32]. A change in the diffusion properties as described above will reflect interaction of the protein with the signalling partner. In other cases, complex formation is required for a protein to participate in specific cellular processes. For example, the membrane protein syntaxin binds to another protein SNAP25 to form an asymmetric complex which is involved in vesicle exocytosis [33]. In both cases, analysis of trajectories will give access to the duration of molecular interactions, thereby providing complementary data to those obtained by observing the average behavior of molecules.

Note added. A few days before submitting the present paper a report was published, dealing with the two-dimensional diffusion of an ellipsoid [34]. The authors solved the Langevin equation, as we did, and they analyzed some statistical quantities at a given time point, such as the second and fourth moments of the displacement of the center of diffusion of the particle.

In our approach, we show how the deviation from the Gaussian behavior can be evidenced by the trajectory of a pointlike marker attached to the diffusing particle at an unknown position. In particular we demonstrate that (1) the diffusion coefficients $(D_{\|}, D_{\perp}, D_{\mathrm{r}})$ can be deduced from the trajectories of the pointlike marker and (2) a few hundred trajectories allows a good estimation of these parameters.

ACKNOWLEDGMENTS

The authors especially acknowledge A. Maggs for informative discussions. This project has been carried out while one of the authors (C.R.) was at the laboratory of Physico-Chimie Theorique at ESPCI as part of the Interdisciplinary Approaches of Life Sciences master program (Paris 5 and Paris 7 Universities and Ecole Normale Superieure). This project was financially supported by the ACI DRAB to one of the authors (A.T.).

APPENDIX A: LANGEVIN EQUATION AND ITS ANALYTICAL SOLUTION

The Langevin equation for the center of diffusion [(1) in the text] can be written in the nondimensionalized matrix form

$$\frac{d\vec{X}_t^{(0)}}{dt} = [\sqrt{2}(1+\eta)^{1/2}\hat{u}_t\hat{u}_t + \sqrt{2}(1-\eta)^{1/2}(\mathbf{1}-\hat{u}_t\hat{u}_t)]\cdot\vec{\Theta}_t, \tag{A1}$$

$$\frac{d\phi_t}{dt} = \sqrt{2}\xi_t, \tag{A2}$$

where the length and time units are ℓ and τ, respectively, and $\hat{u}_t=(\cos\phi_t,\sin\phi_t)^T$ is the unit vector oriented in the longitudinal axis of diffusion associated to $D_{\|}$. In polar coordinates, $(x,y)=r(\cos\theta,\sin\theta)$, the corresponding Fokker-Planck equation for the probability density, $P=P(r,\theta,\phi;t)$ writes as follows:

$$\frac{\partial P}{\partial t} = \left(\nabla\cdot\{(1+\eta)\hat{u}(\phi)\hat{u}(\phi)+(1-\eta)[\mathbf{1}-\hat{u}(\phi)\hat{u}(\phi)]\}\cdot\nabla + \frac{\partial^2}{\partial\phi^2}\right)P, \tag{A3}$$

where $\nabla=(\partial/\partial x,\partial/\partial y)^T$, and $\hat{u}(\phi)=(\cos\phi,\sin\phi)^T$. The above Langevin equation can be integrated analytically, because the orientational degree of freedom $\hat{u}_t$ evolves independently of the translational ones. This is also the case in three dimensions. We may simplify the calculation by introducing the complex notations: $\mathcal{X}_t^{(0)}=X_t^{(0)}+iY_t^{(0)}$ and $\mathcal{X}_t=\mathcal{X}_t^{(0)}+\delta e^{i\phi_t}$ for $\vec{X}_t^{(0)}$ and $\vec{X}_t$ $(\delta=d/\ell)$, respectively, and $d\mathcal{B}_t=dB_{x,t}+idB_{y,t}$ for $\int_t^{t+dt}\vec{\Theta}_s ds$. Here $\mathcal{B}_t$ with $\mathcal{B}_0\equiv 0$ is then a complex Wiener process, satisfying $d\mathcal{B}_s^* d\mathcal{B}_s=2ds$ [35]. (z^* is the complex conjugate of z.) By introducing also a real Wiener process W_t through $dW_t=\int_t^{t+dt}\xi_s ds$, the equations (A1) are solved,

$$\mathcal{X}_t^{(0)} = a\mathcal{B}_t + be^{2i\phi_0}\int_0^t e^{2i\sqrt{2}W_s}d\mathcal{B}_s^*, \tag{A4}$$

where $a=(1+\eta)^{1/2}/\sqrt{2}+(1-\eta)^{1/2}/\sqrt{2}$ and $b=(1+\eta)^{1/2}/\sqrt{2}-(1-\eta)^{1/2}/\sqrt{2}$. The position of the marker is given by

$$\mathcal{X}_t = \mathcal{X}_t^{(0)} + \delta e^{i\phi_0}e^{i\sqrt{2}W_t}. \tag{A5}$$

In order to derive the various statistical averages, we used the formula $\vec{\mathcal{Q}}\cdot\vec{R}=\mathrm{Re}[\mathcal{Q}^*\mathcal{R}]$ that holds for any $\mathcal{Q}=Q_x+iQ_y$, etc. For example, $\hat{u}_{t'}\cdot\hat{u}_t=\mathrm{Re}(e^{-i\sqrt{2}W_{t',t}})$ and the property of the Gaussian stochastic process [35] yields $\langle\mathrm{Re}(e^{-i\sqrt{2}(W_{t'}-W_t)})\rangle=e^{-|t'-t|}$. The calculation can be further simplified when the result does not depend on the initial angle, ϕ_0. For instance, in the calculation of $\langle[\vec{X}_t^{(0)}\cdot\hat{u}_t]^2\rangle$ of (B2), all the terms containing the multiplicative factor $e^{in\phi_0}(n\neq 0)$ can be ignored.

APPENDIX B: ANALYTICAL RESULTS OF STOCHASTIC AVERAGES

In nondimensionalized units, the MSD is

$$\langle|\vec{X}_t-\vec{X}_0|^2\rangle = 4t + 2\delta^2(1-e^{-t}). \tag{B1}$$

There is no sign of the diffusion anisotropy, η. At short time $(t\ll 1)$, the MSD is the sum of the two-dimensional MSD of

the center of diffusion ($4t$) and a term resulting from the displacement of the marker due to the rotation of the particle ($2\delta^2 t$). At long time ($t \gg 1$) only the former contributes to the growth of the MSD, while the additive constant $2\delta^2$ reflects the independent angles of the particle, ϕ_0 and ϕ_t.

The diffusion anisotropy is revealed in the statistical quantities $\hat{C}(t)$ and $C(0,t,t')$, which reflect the translation-rotation coupling and are calculated as

$$\hat{C}(t) \equiv 2\langle[\vec{X}_t^{(0)} \cdot \hat{u}_t]^2\rangle\langle|\vec{X}_t^{(0)}|^2\rangle^{-1} - 1 = \eta(4t)^{-1}(1 - e^{-4t}), \tag{B2}$$

$$C(t',t,0) \equiv 2\langle[(\vec{X}_t - \vec{X}_0) \cdot (\vec{X}_{t'} - \vec{X}_t)]^2\rangle - \langle|\vec{X}_t - \vec{X}_0|^2|\vec{X}_{t'} - \vec{X}_t|^2\rangle = [\eta(1 - e^{-4(t'-t)}) + \delta^2(1 - 2e^{-(t'-t)} + e^{-4(t'-t)})] \times [\eta(1 - e^{-4t}) + \delta^2(1 - 2e^{-t} + e^{-4t})]. \tag{B3}$$

At small time $t \ll 1$, the average $C(0,t,2t)$ increases as $16(\eta - \delta^2/2)^2 t^2$, and finally tends to a constant, $C(0,t,t') \simeq (\eta + \delta^2)^2$ at $t \gg 1$ and $(t'-t) \gg 1$. We note that the following simple relationship holds:

$$\langle|\vec{X}_t - \vec{X}_0|^2|\vec{X}_{t'} - \vec{X}_t|^2\rangle = \langle|\vec{X}_t - \vec{X}_0|^2\rangle\langle|\vec{X}_{t'} - \vec{X}_t|^2\rangle, \tag{B4}$$

which is not evident knowing that the displacement vectors $\vec{X}_t - \vec{X}_0$ and $\vec{X}_{t'} - \vec{X}_t$ are correlated through the orientation of the object at time t.

The effect of anisotropy also appears in the fourth order moment of the displacement,

$$\langle|\vec{X}_t - \vec{X}_0|^4\rangle = 32t^2 + 32\delta^2 t(1 - e^{-t}) + \delta^4(6 - 8e^{-t} + 2e^{-4t}) + \eta^2(1 - e^{-4t})^2 + 4\delta^2\eta(1 - e^{-4t} - 4te^{-t}). \tag{B5}$$

This shows the non-Gaussian nature of the displacement, $\vec{X}_t - \vec{X}_0$: even with $\delta = 0$ the equality of the two-dimensional random walk, $\langle|\vec{X}_t - \vec{X}_0|^4\rangle = 2\langle|\vec{X}_t - \vec{X}_0|^2\rangle^2$, is not recovered.

APPENDIX C: NUMERICAL METHOD FOR SIMULATING LANGEVIN EQUATION

We have used the Heun's method, which is an improved version of the second order Runge-Kutta method. With a given nondimensionalized time step Δt, the update of the present position, $\vec{X}_{n\Delta t}$, and that of the angle, $\phi_{n\Delta t}$, at the discretized time $n\Delta t$ ($n \geq 0$) are, respectively, given as follows:

$$\vec{X}_{(n+1)\Delta t} = \vec{X}_{n\Delta t} + \frac{1}{2}(\mathcal{M}_{(n+1)\Delta t} + \mathcal{M}_{n\Delta t}) \cdot \Delta B_{n+1},$$

$$\phi_{(n+1)\Delta t} = \phi_{n\Delta t} + \sqrt{2}\Delta W_{n+1}, \tag{C1}$$

where $\mathcal{M}_t$ is the 2×2 matrix defined as

$$\mathcal{M}_t = \sqrt{2}(1 + \eta)^{1/2}\hat{u}_t\hat{u}_t + \sqrt{2}(1 - \eta)^{1/2}(\mathbf{1} - \hat{u}_t\hat{u}_t), \tag{C2}$$

and $\{\Delta B_1, \Delta B_2, \ldots,\}$ and $\{\Delta W_1, \Delta W_2, \ldots\}$ are the independent Gaussian random numbers obeying the standard normal distributions, i.e., $\langle \Delta B_n \rangle = 0$ and $\langle \Delta B_n^2 \rangle = 1$, etc.

In the Heun's scheme, the truncation error due to the temporal discretization of the Langevin equation varies as n^{-2} at each time step, where n is the number of divisions of a given time interval t of calculation (i.e., $\Delta t = t/n$). This method, therefore, results in a maximum error of $\sim n^{-1}$ through the entire interval (see, for example, Ref. [36]). For the time span of $t \sim \tau/2$, the time step of $\Delta t < \tau/600$ was sufficient for the purpose of distinguishing different values of the anisotropy parameter, η (see the figures in the text).

[1] B. J. Berne and R. Pecora, *Dynamic Light Scattering: With Applications to Chemistry, Biology, and Physics* (Dover, New York, 2000).
[2] J. S. Higgins and H. C. Benoit, *Polymers and Neutron Scattering* (Oxford University Press, Oxford, 1997).
[3] N. J. Reits and J. J. Neefjes, Nat. Cell Biol. **3**, E145 (2001).
[4] S. P. Bacia and P. Schwille, Methods **29**, 74 (2003).
[5] H. Geerts, M. De Brabander, R. Nyudens, S. Geuens, J. D. M. Moeremans, and P. Hollenbeck, Biophys. J. **52**, 775 (1987).
[6] M. J. Saxton and K. Jacobson, Annu. Rev. Biophys. Biomol. Struct. **26**, 373 (1997).
[7] A. Kusumi, C. Nakada, K. Ritchie, K. Murase, K. Suzuki, H. Murakoshi, R. S. Kasai, J. Kondo, and T. Fujiwara, Annu. Rev. Biophys. Biomol. Struct. **35**, 351 (2005).
[8] M. Dahan, S. Lévi, C. Luccardini, P. Rostaing, B. Riveau, and A. Triller, Science **302**, 442 (2003).
[9] P. G. Saffman and M. Delbrück, Proc. Natl. Acad. Sci. U.S.A. **72**, 3111 (1975).
[10] Y. Gambin, R. Lopez-Esparza, M. Reffay, E. Sierecki, N. S. Gov, M. Genest, R. S. Hodges, and W. Urbach, Proc. Natl. Acad. Sci. U.S.A. **103**, 2098 (2006).
[11] A. J. Levine, T. B. Liverpool, and F. C. MacKintosh, Phys. Rev. E **69**, 021503 (2004).
[12] F. Perrin, J. Phys. Radium **5**, 497 (1934).
[13] F. Perrin, J. Phys. Radium **7**, 1 (1936).
[14] R. Pecora, J. Chem. Phys. **40**, 1604 (1964).
[15] L. I. Komarov and I. Z. Fisher, Zh. Eksp. Teor. Fiz. **43**, 1927 (1962).
[16] H. Maeda and N. Saitô, J. Phys. Soc. Jpn. **27**, 984 (1969).
[17] S. H. Harvey and J. García de la Torre, Macromolecules **13**, 960 (1980).
[18] Y.-G. Tao, W. K. den Otter, J. T. Padding, J. K. G. Dhont, and W. J. Briels, J. Chem. Phys. **122**, 244903 (2005).
[19] T. Nakata, R. Saito-Yoshitake, Y. Okada, and N. Hirokawa, Biophys. J. **65**, 2504 (1993).
[20] M. X. Fernandes and J. García de la Torre, Biophys. J. **83**,

3039 (2002).
[21] X. Brokmann, M.-V. Ehrensperger, J.-P. Hermier, A. Triller, and M. Dahan, Chem. Phys. Lett. **406**, 210 (2005).
[22] M. Y. Ali, K. Homma, A. Hikikoshi-Iwane, K. Adachi, H. Itoh, K. Kinosita Jr., T. Yanagida, and M. Ikebe, Biophys. J. **86**, 3804 (2004).
[23] M. M. Krishna and A. S. N. Periasamy, Biophys. Chem. **90**, 123 (2001).
[24] S. H. Park, A. A. Mrse, A. A. Nevzorov, A. A. D. Angelis, and S. J. Opella, J. Magn. Reson. **178**, 162 (2006).
[25] T. Fujiwara, K. Ritchie, H. Murakoshi, and K. J. A. Kusumi, J. Cell Biol. **157**, 1071 (2002).
[26] K. I. Willig, R. R. Kellner, R. Medda, B. Hein, S. Jakobs, and S. W. Hell, Nat. Methods **3**, 721 (2006).
[27] M. Nishiyama, E. Muto, Y. Inoue, T. Yanagida, and H. Higuchi, Nat. Cell Biol. **3**, 425 (2001).
[28] M. Edidin, Trends Cell Biol. **11**, 492 (2001).
[29] S. Khan, A. M. Reynolds, I. E. G. Morrison, and R. J. Cherry, Phys. Rev. E **71**, 041915 (2005).
[30] A. Moreno and W. Kob, J. Chem. Phys. **121**, 380 (2004).
[31] A. Moreno and W. Kob, Philos. Mag. **84**, 1383 (2004).
[32] R. M. Lindsay, Philos. Trans. R. Soc. London, Ser. B **351**, 365 (1996).
[33] J. B. Sorensen, Trends Neurosci. **28**, 453 (2005).
[34] Y. Han, A. M. Alsayed, M. Nobili, J. Zhang, T. C. Lubensky, and A. G. Yodh, Science **314**, 626 (2006).
[35] C. W. Gardiner, *Handbook of Stochastic Methods: For Physics, Chemistry and the Natural Sciences*, 3rd ed. (Springer, New York, 2004).
[36] M. T. Heath, *Scientific Computing, An Introductory Survey (Section 9.3.7.)*, 2nd ed. (McGraw-Hill, New York, 2002).